

Experiment and optimization of the potato-soil separation and conveying device for a harvester using RecurDyn-EDEM coupling simulation

Yongfei Pan^{1,2,3}, Ranbing Yang^{2,3*}, Huan Zhang⁴, Jian Zhang^{2,3},
Xiantao Zha^{2,3}, Zhuchuan Qiu^{1,2}, Minsheng Wu^{2,3}

(1. College of Information and Communication Engineering, Hainan University, Haikou 570228, China;

2. College of Mechanical and Electrical Engineering, Hainan University, Haikou 570228, China;

3. Key Laboratory of Tropical Intelligent Agricultural Equipment, Ministry of Agriculture and Rural Affairs, Danzhou 571700, China;

4. College of Mechanical and Electrical Engineering, Qingdao Agricultural University, Qingdao 266109, China)

Abstract: To address issues such as suboptimal separation of potatoes from soil during harvest, weak damage prevention and reduction capabilities in the transport process, and high damage rates, a potato-soil-transport device motion model was proposed based on potato farming practices in northern China (Gansu). The mechanical properties of the separation and transport device and the movement mechanism of the potatoes were analyzed, identifying key factors affecting the separation efficiency of potatoes from soil and potato damage: separation transport device inclination angle (a), machine forward speed (V_m), paddle wheel amplitude (A), and paddle wheel frequency (f). A coupled RecurDyn-EDEM simulation model was constructed to determine the impact of key factors on soil separation efficiency and potato damage. Using an optimization method, the optimal parameter combination for evaluating potato-soil separation was determined: separation transport device inclination angle of 18°, machine forward speed of 4.7 km/h, paddle wheel amplitude of 32.8 mm, and paddle wheel frequency of 6.0 Hz. Field tests showed that the potato-soil separation efficiency was good, with potatoes containing minimal soil and other impurities and experiencing minimal damage. The average potato-soil separation efficiency was 96%, and the average potato damage rate was 2%. Compared to the simulation results, the errors were 0.47% and 0.3%, respectively, meeting the quality requirements for potato harvesting operations.

Keywords: potato, separation and transport, coupled simulation, experiment

DOI: [10.25165/j.ijabe.20251804.9219](https://doi.org/10.25165/j.ijabe.20251804.9219)

Citation: Pan Y F, Yang R B, Zhang H, Zhang J, Zha X T, Qiu Z C, et al. Experiment and optimization of the potato-soil separation and conveying device for a harvester using RecurDyn-EDEM coupling simulation. Int J Agric & Biol Eng, 2025; 18(4): 149–156.

1 Introduction

Potatoes are the fourth largest staple crop in China, widely cultivated due to their drought resistance, cold tolerance, and broad adaptability. In 2022, the potato planting area in China was 7185000 hm²^[1]. As the potato industry continues to evolve, there has been an increase in the proportion of potatoes grown for fresh consumption, which has led to new demands for low-damage harvesting processes. Freshly consumed potatoes require minimal damage and effective soil separation. Currently, much research focuses on soil-potato separation in clay and sandy soils, yet there is a lack of studies specifically addressing loess soils in Gansu^[2-7].

Gansu, representing one of China's primary potato-growing regions, features hilly terrain with loess soil - a mixture of loam and clay known for its excellent water and fertilizer retention. During

the potato harvesting season, the soil's adhesiveness increases with the rain, causing clay to adhere to the potato surfaces, making them difficult to detach. Enhancing the effectiveness of soil-potato separation in loess soils within Gansu is crucial to ensuring damage-free potato harvesting^[8-13].

The inclined vibrating bar chain separation and conveyance device is a key component of combined potato harvesters. It improves soil-potato separation efficiency through its angled vibration mechanism^[14]. Researchers both domestically and internationally have optimized the structure and parameters of potato harvesters' soil separation conveyance chains. Innovations include adding auxiliary vibration mechanisms and wave-shaped soil separation structures, and optimizing the angle of the lifting chain to enhance separation effectiveness^[15-17].

Wei et al.^[18] developed a wave-shaped soil separation device based on discrete element modeling that employs both vibration and wave motions to achieve remarkable soil separation and damage reduction results. Yang et al.^[19] designed a high-low interval dual-stage conveyance separation device, which, based on orthogonal rotational combination tests and field experiments, identified optimal operating parameters: a line speed of 0.6 m/s, an amplitude of 26.2 mm, and a frequency of 6.6 Hz. Chen et al.^[20] and others proposed an RVPSD potato separation device. Through simulation experiments, the optimal working parameters for RVPSD were determined as the vibration point position, potato-soil separation lifting chain speed, rotor amplitude, and rotor vibration frequency, which are 646.5 mm, 1.08 m/s, 26.7 mm, and 5.9 Hz, respectively.

Received date: 2024-07-11 Accepted date: 2025-05-26

Biographies: **Yongfei Pan**, PhD candidate, research interest: intelligent agricultural equipment, Email: panyongfei@163.com; **Huan Zhang**, research interest: intelligent agricultural equipment, Email: 200501102@qau.edu.cn; **Jian Zhang**, research interest: intelligent agricultural equipment, Email: zhangjian_qau@163.com; **Xiantao Zha**, research interest: intelligent agricultural equipment, Email: zhaxt@hainanu.edu.cn; **Zhuchuan Qiu**, research interest: intelligent agricultural equipment, Email: 1252750182@qq.com; **Minsheng Wu**, research interest: intelligent agricultural equipment, Email: wms22336@163.com.

***Corresponding author:** Ranbing Yang, PhD, Professor, The Yangtze River Scholar, research interest: intelligent agricultural equipment. College of Mechanical and Electrical Engineering, Hainan University, Haikou 570228, China. Tel: +86-13646422839, Email: yangranbing@163.com.

Wang et al.^[21] designed a simple harmonic disturbance separation device for a potato harvester. Through coupled simulation, the optimal operating speed for the separation screen of the harvester was determined to be 0.7 m/s, with a disturbance depth of 51.5 mm, paddle wheel speed set to 2.3 r/s by a regulator, and an eccentric distance of 31 mm, achieving a soil clod crushing rate of 60.7%. The Gansu Provincial Agricultural Mechanization Technology Extension Center optimized the vibratory separation screen structure of potato harvesters for cohesive soils in the Loess Plateau region of Gansu Province. By proposing a parameter combination of linear velocity (0.8–2.2 m/s) for the separation screen, the skin breakage rate and tuber damage rate were significantly reduced. However, critical parameters such as vibration amplitude and tilt angle were not investigated^[22]. In addition, Feng et al.^[23] from Gansu Agricultural University conducted a kinematic analysis on the separation screen and potato tubers of small-scale potato harvesters tailored to the potato cultivation conditions in Dingxi City, Gansu Province, to determine key operational parameters for the separation process. However, only rough ranges were provided without specifying parameters for particular soil conditions.

A research team from Russia designed a multi-cam vibrator installed on a potato-soil separation device. Through bench tests, the optimal rotational speed was determined to be 130 r/min, and the best vibration frequency was 2.2 Hz^[24]. A research team from Ukraine designed a rotary clod-breaking method. With a soil moisture content of 18.4%, the optimal rotor rotational frequency and translation speed were 100 min⁻¹ and $V_m=1.5$ m/s, respectively, achieving a soil separation efficiency of 93.5%^[25]. Issa et al.^[26] optimized a potato-soil conveying separation mechanism. Through field experiments, the optimal conveying speed of the potato-soil separation lifting chain and the machine forward speed were determined to be 4 km/h and 6.5 km/h, respectively. Lü et al.^[27] designed a vibrating potato-soil separation device for sticky heavy soil. Based on actual working soil conditions and theoretical analysis, the working amplitude of the vibrator was determined to be 60 mm, with a frequency of $f=6$ Hz. The above studies mainly focus on vibration frequency, amplitude, and rotational speed, without considering the inclination angle, machine forward speed, and their proportional relationships.

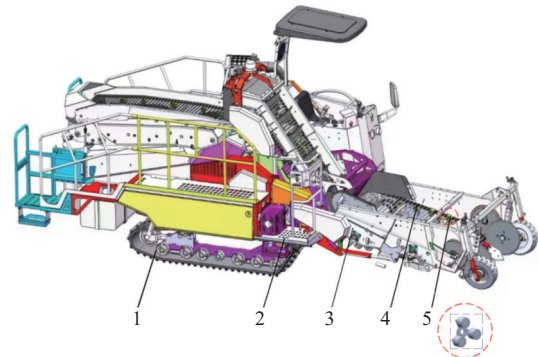
Considering the influence of tilt angle, frequency, amplitude, and forward speed on the potato-soil separation device, a mechanical model of potato-soil separation and transportation was established. Based on this model, the value ranges for tilt angle, frequency, amplitude, and forward speed were determined. Using a coupled simulation model of potato-soil separation designed with RecurDyn-EDEM simulation, the Design-Expert 12 software was utilized to design and simulate coupled experiments. The optimal parameter combination was obtained and verified through prototype field tests.

2 Mechanical model of vibration conveyance in potato-soil separation process

2.1 Overall machine design and working principle

The self-propelled potato combine harvester is shown in Figure 1. The potato-soil separation and conveying device is located at the front of the machine and consists of a vibrating conveyor chain, beaters, and baffles. The beaters are installed on both sides of the vibrating conveyor chain and are powered by a hydraulic motor. Each rotation of the beaters allows for three beating actions on the vibrating conveyor chain, thereby inducing vibration. During

operation, the dug-up potatoes and soil enter the potato-soil separation and conveying device, where the vibrating conveyor chain facilitates the separation of potatoes from the soil. The separated potatoes then enter the lifting device, while the soil falls through the potato-soil separation conveyor chain and drops beneath the machine.



1. Power unit 2. Manual observation platform 3. Baffle 4. Vibrating conveyor chain 5. Paddle wheel

Figure 1 Overall machine structure diagram

2.2 Mechanical model of the soil-potato separation conveyance unit

The primary sources of potato damage and soil-potato separation issues stem from collisions between the potatoes and the vibrating conveyor chain. The equation describing the contact force between the potatoes and the vibrating conveyor chain is:

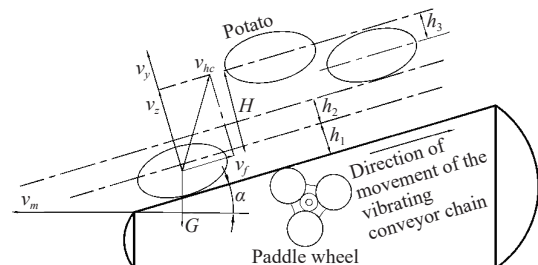
$$F = P * S \quad (1)$$

where, F represents the contact force of the potato collision, N ; P denotes the contact stress between the potato and the vibrating conveyor chain, N ; S is the contact area between the potato and the vibrating conveyor chain, mm^2 .

Based on the literature^[28], the relationship between the potato collision contact area S and the drop height h_3 is given as follows:

$$S = 897.3h_3 + 122.2 \quad (2)$$

This equation demonstrates validity for Longshu potatoes with mass parameters ranging from 150 to 250 g under impact loading conditions between tuber specimens and nitrile rubber (NBR) interfaces. Consequently, a bouncing collision model for potatoes has been established. The model is shown in Figure 2.



Note: v_m is the forward speed of the machine, m/s; v_f is the speed of the conveyor belt, m/s; α is the angle of inclination of the conveyor belt, ($^{\circ}$); v_y is the vertical speed of the potato relative to the conveyor chain, m/s; v_x is the initial velocity of the potato after collision, m/s, and the direction is the same as v_y , perpendicular to the conveyor chain; H is the vertical height the potato rises on the conveyor belt, m; h_1 is the vertical height from the screen at which the potato chunk reaches its maximum height, m; h_2 is the vertical height the potato rises as it falls along the screen, m; h_3 is the vertical height of the potato as it falls along the screen, m^[29].

Figure 2 Velocity decomposition of clamping carrier

The potatoes move linearly upwards and reach their highest point due to the vibration caused by the beaters striking the conveyor belt. During this process, the machine continues to move forward, causing the conveyor chain to move a distance h_1 in the forward direction, while the conveyor chain itself moves a distance h_2 . The equation can be expressed as:

$$\begin{cases} h_1 = v_m t_1 \cos \alpha \\ h_2 = v_m t_2 \cos \alpha \\ h_3 = \frac{1}{2} g t^2 \cos \alpha \\ t_1 = \frac{v_y}{g \cos \alpha} \end{cases} \quad (3)$$

where, t_1 represents the time it takes for the potato to reach its maximum height. Combining the above expressions yields:

$$h_3 = \frac{(v_z + v_m \sin \alpha)^2}{2g \cos \alpha} \left(\frac{h_2}{h_1} \right)^2 \quad (4)$$

From the motion analysis, we derive:

$$v_z = A\omega_f \sin(\omega_f t + P) \quad (5)$$

By calculating Equations (3) and (5), the vertical height of the potato's fall along the screen surface can be expressed as:

$$h_3 = \frac{[A\omega_f \sin(\omega_f t + P) + v_m \sin \alpha]^2}{2g \cos \alpha} \left(\frac{h_2}{h_1} \right)^2 \quad (6)$$

Substituting Equation (6) into Equation (2) yields the collision contact force relationship, which can be expressed as:

$$F = 897.3 \frac{[A\omega_f \sin(\omega_f t + P) + v_m \sin \alpha]^2}{2g \cos \alpha} \left(\frac{h_2}{h_1} \right)^2 + 112.20 \quad (7)$$

According to Equation (7), the collision of potatoes is primarily influenced by the inclination angle (α) of the vibrating conveyor chain relative to the ground, the forward speed (v_m) of the machine, and the angular velocity (ω) of the paddle wheel, which directly affects the vibration frequency. Therefore, the inclination angle (α), machine forward speed (v_m), paddle wheel amplitude, and paddle wheel vibration frequency are selected as experimental factors for testing.

3 Coupled simulation and analysis

3.1 Coupling of RecurDyn and EDEM models

The secondary potato-soil separation device was simplified by removing the redundant parts except for the roller group, to eliminate interference factors and reduce the computational load of the simulation. Secondary modeling was performed using SolidWorks, and the simplified conveyor device created in SolidWorks was saved in *.xt* format and imported into RecurDyn.

In RecurDyn, the motion model for the conveyor device was set up. The inclination angle of the model was adjusted to change the tilt angle of the vibrating conveyor chain, the rotational speed of the drive wheel was altered to adjust the forward speed of the machine, the relative position of the beaters to the conveyor chain was adjusted to regulate the amplitude, and the beaters themselves were adjusted to control the vibration frequency. After setting up the drives, contacts, constraints, and angles, the simulation was run and the results were exported as *.wall* format files and imported into EDEM.

In EDEM, the parameters for the soil and potatoes were set, with the LongShu-12 potato variety selected as the test object. The potato's external contour was obtained through 3D scanning, and in

EDEM, the potato simulation model was created using particle filling, as shown in Figure 3. Using EDEM-Properties, the filled potato's weight was calculated to be 0.4 kg, resulting in a gravitational force $G = 3.92$ N.



Figure 3 Potato model

To improve computational efficiency, the soil particle radius was set to 5 mm, and the soil was modeled as bonding. Using the built-in particle units in EDEM, four different types of soil particles were established: spherical block particles, cylindrical particles, block particles, and core particles, as shown in Figure 4.

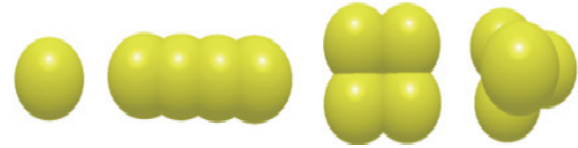


Figure 4 Soil particle model

Based on potato planting agronomy, the distribution of potatoes in the soil is set to a double-row ridge, with a plant spacing of 200 mm front-to-back and 250 mm left-to-right. Five potatoes per plant are randomly distributed in the ridge soil. Some soil adheres to the surface of the potatoes to simulate the soil-tuber separation effect under clay conditions, as shown in Figure 5.

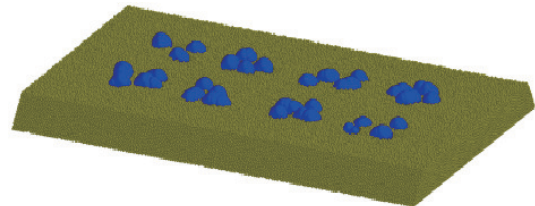


Figure 5 Distribution of potatoes in the soil

Equipment materials and geometries are set, and soil transport parts, baffles, and collection boxes are added to the model. The settings include Number of Cells as 743 256, Fix Time Step as 6e-06 s, required iterations as 1.67e+06s, save time as 0.01 s, and total time as 10 s, as shown in Figure 6.

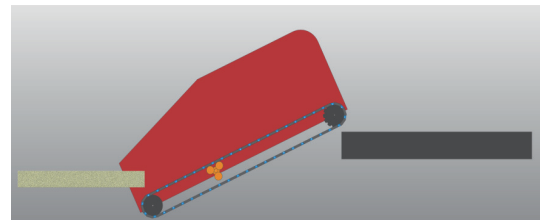


Figure 6 Coupling of RecurDyn and EDEM models

The soil parameters are shown in Table 1, and the contact between particles uses the *Hertz-Mindlin (no slip)* model. The necessary parameters for discrete element simulation were determined through field soil tests and literature review^[30-34], as listed in Table 1.

Table 1 Parameters of discrete element simulation model

Parameter	Value
Soil trough size (length×width×height)/mm	1000×800×120
Potato planting depth/mm	10
Number of potatoes per plant	5
Number of potato plants	8
Soil particle density/kg·m ⁻³	1360
Poisson's ratio of soil	0.40
Soil shear modulus/MPa	1
Coefficient of restitution between soil particles	0.60
Static friction coefficient between soil particles	0.45
Dynamic friction coefficient between soil particles	0.21
Poisson's ratio of potato	0.33
Potato density/kg·m ⁻³	1068
Shear modulus of potato/MPa	0.75
Coefficient of restitution between potato and soil	0.46
Static friction coefficient between potato and soil	0.41
Dynamic friction coefficient between potato and soil	0.06
Recovery coefficient between soil and 65Mn	0.30
Static friction coefficient between soil and 65Mn	0.50
Dynamic friction coefficient between soil and 65Mn	0.05
Particle filling radius/mm	5
Simulation time/s	10

The model for the interaction between potatoes and soil particles is set to the Hertz-Mindlin with Bonding model. When the normal and shear stresses exceed the model parameters, the bond breaks^[35], that is:

$$\sigma_{\max} < \frac{-F_n}{A} + \frac{2M_t}{J}R_B \quad (8)$$

$$\tau_{\max} < \frac{-F_t}{A} + \frac{M_n}{J}R_B \quad (9)$$

3.2 Experimental design and simulation results

According to Equation (7), the primary factors affecting soil-potato separation are identified as: inclination angle of the vibrating conveyor chain (X_1), machine forward speed (X_2), paddle wheel amplitude (X_3), and paddle wheel frequency (X_4). These factors were selected for experimentation based on the design requirements of the self-propelled combined harvester. The inclination angle of the vibrating conveyor chain α is set between 12°-20°, and the machine forward speed is between 3 km/h-7 km/h. Referring to the literature^[35], the paddle wheel amplitude is selected from 10 mm to 50 mm, and the paddle wheel frequency range is from 5 Hz to 9 Hz. Soil content and damage rate are chosen as evaluation indicators. A four-factor, five-level orthogonal combination simulation experiment is designed using Design-Expert 12 software. The factors and their level coding are presented in Table 2.

Table 2 Factor and level coding table of digging resistance test

Code	Experimental Factors			
	Inclination angle/(°)	Speed/km·h ⁻¹	Amplitude/mm	Frequency/Hz
-2	12	3	10	5
-1	14	4	20	6
0	16	5	30	7
1	18	6	40	8
2	20	7	50	9

Simulation results indicate that the primary mechanisms for separating potatoes from adhesive soil involve collisions between potatoes themselves and between potatoes and the vibrating conveyor chain. After the potato-soil composite enters the vibrating conveyor chain, gravity causes the soil to fall through the gaps in the conveyor, as shown in Figure 7. By 2.0 seconds, most of the soil has been removed, as shown in Figure 8.

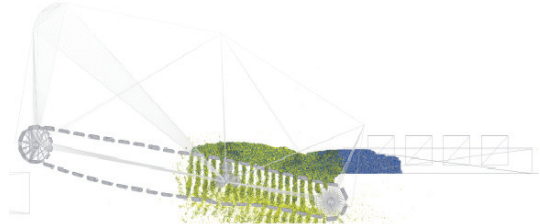


Figure 7 Soil begins to fall



Figure 8 Complete soil detachment

By setting the “Potato-Smooth Color by Velocity and levels three” in the Analyst Tree-Particle, the movement speed of the potatoes is displayed, showing that under the transport of the vibrating conveyor chain, the trajectory of the potatoes is thrown backward diagonally, while the soil continues to fall beneath the machine, as shown in Figure 9.

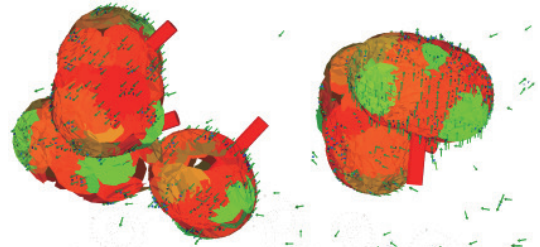


Figure 9 Potato movement trajectory

In Analyst Tree-Particle, under the “Total Force” settings for Potato and Soil, it is evident that the soil on the potato surface, influenced by the interaction between the potato and the vibrating conveyor chain, experiences forces along the surface of the potato. When these forces reach the deformation limit of the bonding, the soil surface begins to disintegrate. The bond does not continue to break until the stress returns to a sustainable range. However, a small amount of soil particles remain adhered to the potato surface, making subsequent collisions insufficient to separate the clinging soil from the potatoes, as shown in Figure 10. The test results are listed in Table 3.

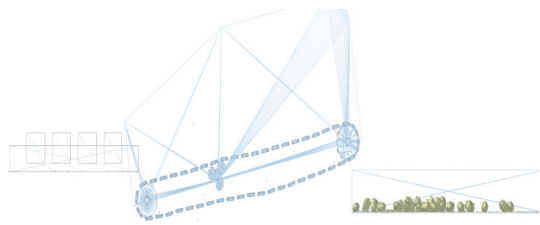


Figure 10 Simulation completed

Table 3 Scheme and results of potato-soil separation test

No.	Experimental factors				Response	
	X_1	X_2	X_3	X_4	$Y_1/\%$	$Y_2/\%$
1	14	4	20	6	91.98	1.66
2	18	4	20	8	89.78	2.01
3	16	3	30	7	94.88	1.48
4	18	4	40	8	88.31	2.97
5	16	3	50	7	90.56	2.59
6	14	4	40	6	95.95	2.07
7	18	2	40	6	96.46	2.04
8	14	4	40	8	91.97	2.17
9	16	3	30	7	96.58	1.26
10	18	4	20	6	92.07	2.03
11	18	2	20	6	93.01	1.68
12	14	4	20	8	92.31	1.75
13	16	3	30	7	95.02	1.18
14	12	3	30	7	97.51	1.52
15	16	3	30	9	95.45	1.5
16	14	2	20	8	93.81	1.08
17	16	5	30	7	90.2	2.5
18	18	2	40	8	94.26	2.01
19	18	2	20	8	91.82	1.56
20	14	2	20	6	91.85	1.78
21	14	2	40	8	93.26	2.03
22	16	3	30	7	95.69	1.35
23	16	3	30	5	97.04	1.95
24	20	3	30	7	93.69	1.82
25	16	3	30	7	94.98	1.49
26	16	3	10	7	88.81	1.7
27	16	3	30	7	95.61	1.3
28	14	2	40	6	96.48	1.8
29	18	4	40	6	93.01	2.11

3.3 Regression equation and analysis of experimental results

Variance analysis was conducted using Design Expert 12 software. By analyzing the variances within and between groups,

we can determine whether the data from each group comes from populations with the same mean. The coefficient p can be used to judge whether these differences are statistically significant. The model is significant ($p < 0.0001$) and the lack-of-fit terms are not significant ($p > 0.1$), indicating that the model is effective. All quadratic regression models are significant ($p < 0.05$), and the regression equations have no lack of fit, indicating a good fit of the model to the samples.

Table 4 shows that the p -value of rotational speed X_2 for the soil content rate Y_1 is less than 0.0001, indicating that the rotational speed has a highly significant effect on the soil content rate. The p -value of rotational speed X_3 for the damage rate Y_2 is less than 0.0001, indicating that the rotational speed has a highly significant effect on the damage rate. From the F -values, the order of influence on the soil content rate Y_1 is as follows: machine forward speed (X_2) > paddle wheel frequency (X_4) > paddle wheel amplitude (X_3) > inclination angle of the vibrating conveyor chain (X_1). The order of influence on the damage rate Y_2 is as follows: paddle wheel amplitude (X_3) > paddle wheel frequency (X_4) > machine forward speed (X_2) > inclination angle of the vibrating conveyor chain (X_1).

With an analysis of experimental results and multiple regression fitting, the quadratic equations of multiple regression for inclination angle, machine forward speed, rotor amplitude, and rotor vibration frequency with soil content rate and damage rate were obtained:

$$Y_1 = 95.46 - 0.6888x_1 - 0.9588x_2 + 0.6904x_3 - 0.7696x_4 - 0.5744x_1x_2 - 0.8069x_3x_4 - 0.9336x_2^2 - 1.53x_3^2$$

$$Y_2 = 1.34 + 0.1029x_1 + 0.1179x_2 + 0.1846x_3 - 0.0871x_4 + 0.1781x_2x_4 + 0.1819x_3x_4 + 0.0966x_1^2 + 0.2266x_2^2 + 0.2153x_3^2 + 0.1103x_4^2$$

3.4 Analysis of the effects of interaction terms on experimental indicators

The response surface, as shown in **Figure 11**, reveals that different factor values have varying impacts on the final results.

Table 4 Analysis of variance

Source	Soil content					Damage rate				
	Sum of squares	Mean square	df	F	p	Sum of squares	Mean square	df	F	p
Model	166.85	11.92	14	15.30	< 0.0001***	5.24	0.3745	14	15.23	< 0.0001***
x_1	11.39	11.39	1	14.62	0.0017**	0.2542	0.2542	1	10.34	0.0058**
x_2	22.05	22.05	1	28.32	< 0.0001***	0.3337	0.3337	1	13.57	0.0022**
x_3	11.44	11.44	1	14.69	0.0016**	0.8177	0.8177	1	33.25	< 0.0001***
x_4	14.21	14.21	1	18.25	0.0007**	0.1820	0.1820	1	7.40	0.0158**
x_1x_2	5.28	5.28	1	6.78	0.0200**	0.0281	0.0281	1	1.14	0.3024
x_1x_3	0.3452	0.3452	1	0.4431	0.5157	0.0077	0.0077	1	0.3113	0.5851
x_1x_4	1.87	1.87	1	2.40	0.1421	0.0856	0.0856	1	3.48	0.0819
x_2x_3	2.95	2.95	1	3.79	0.0706	0.0298	0.0298	1	1.21	0.2887
x_2x_4	2.24	2.24	1	2.88	0.1104	0.5077	0.5077	1	20.64	0.0004**
x_3x_4	10.42	10.42	1	13.37	0.0023**	0.5293	0.5293	1	21.52	0.0003**
x_1^2	0.0649	0.0649	1	0.0833	0.7768	0.2558	0.2558	1	10.40	0.0057**
x_2^2	23.91	23.91	1	30.69	< 0.0001***	1.41	1.41	1	57.24	< 0.0001***
x_3^2	63.99	63.99	1	82.15	< 0.0001***	1.27	1.27	1	51.70	< 0.0001***
x_4^2	0.3478	0.3478	1	0.4465	0.5142	0.3338	0.3338	1	13.57	0.0022**
Residual	11.68	0.7790	15			0.3689	0.0246	15		
Lack of fit	9.59	0.9594	10	2.30	0.1859	0.2932	0.0293	10	1.94	0.2414
Pure error	2.09	0.4180	5			0.0757	0.0151	5		
Cor total	178.53		29			5.61		29		

Note: *** indicates extremely significant ($p < 0.0001$); ** indicates significant ($0.0001 < p < 0.05$).

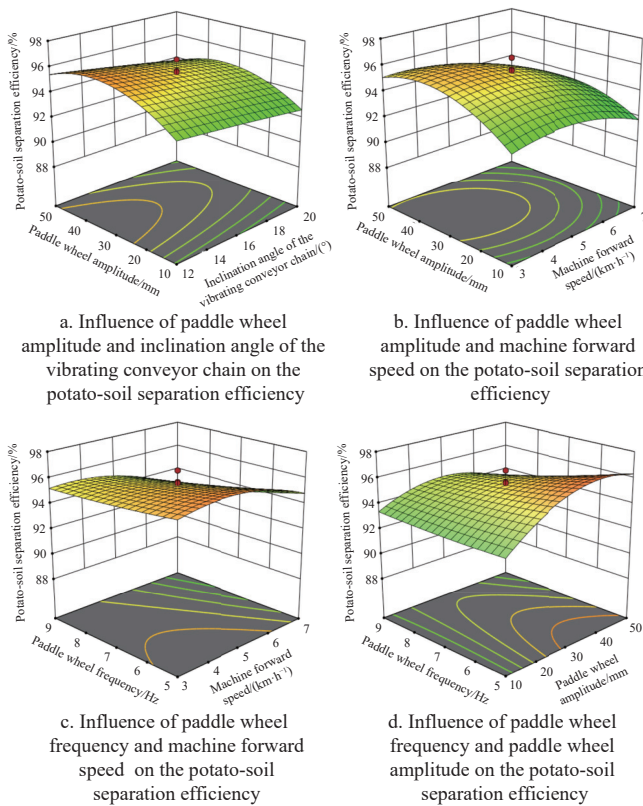


Figure 11 Two-factor influence response surface for potato-soil separation efficiency

As shown in Figure 11a, when the inclination angle of the vibrating conveyor chain increases from 12° to 20°, the potato-soil separation efficiency shows a slight decreasing trend. From Figures 11b and 11c, it can be seen that when the machine forward speed increases from 3 to 7 km/h, the potato-soil separation efficiency first increases and then decreases. From Figures 11b and 11d, it can be seen that when the paddle wheel amplitude increases from 10 to 50 mm, the potato-soil separation efficiency first increases and then decreases. From Figures 11c and 11d, it can be seen that when the paddle wheel frequency increases from 5 to 9 Hz, the potato-soil separation efficiency shows a slight decreasing trend.

As shown in Figures 12a and 12b, when the inclination angle of the vibrating conveyor chain increases from 12° to 20°, the potato damage rate first decreases and then increases. From Figure 12c, it can be seen that when the machine's forward speed increases from 3 to 7 km/h, the potato damage rate first decreases and then increases. From Figures 12c and 12d, it can be seen that when the paddle wheel amplitude increases from 10 to 50 mm, the potato damage rate first increases and then decreases. As shown in Figure 12d, when the paddle wheel frequency increases from 5 to 9 Hz, the potato damage rate shows a decreasing trend.

In addressing low-dimensional objective optimization problems, the NSGA-II algorithm^[36,37] was used in combination with objective functions and constraints to obtain the optimal operating parameters for the harvester:

$$\begin{cases} \max Y_1(X_1 X_2 X_3 X_4), \min Y_2(X_1 X_2 X_3 X_4) \\ 12^\circ \leq X_1 \leq 20^\circ, 3 \text{ km/h} \leq X_2 \leq 7 \text{ km/h} \\ 10 \text{ mm} \leq X_3 \leq 50 \text{ mm}, 5 \text{ Hz} \leq X_4 \leq 9 \text{ Hz} \end{cases}$$

After running the NSGA-II algorithm, the optimal operating parameters for potato-soil separation-inclination angle of the

vibrating conveyor chain, machine forward speed, paddle wheel amplitude, and paddle wheel frequency are determined to be 18°, 4.739 km/h, 32.835 mm, and 6.004 Hz, respectively. Correspondingly, the potato-soil separation efficiency is 96.47%, and the potato damage rate is 1.70%.

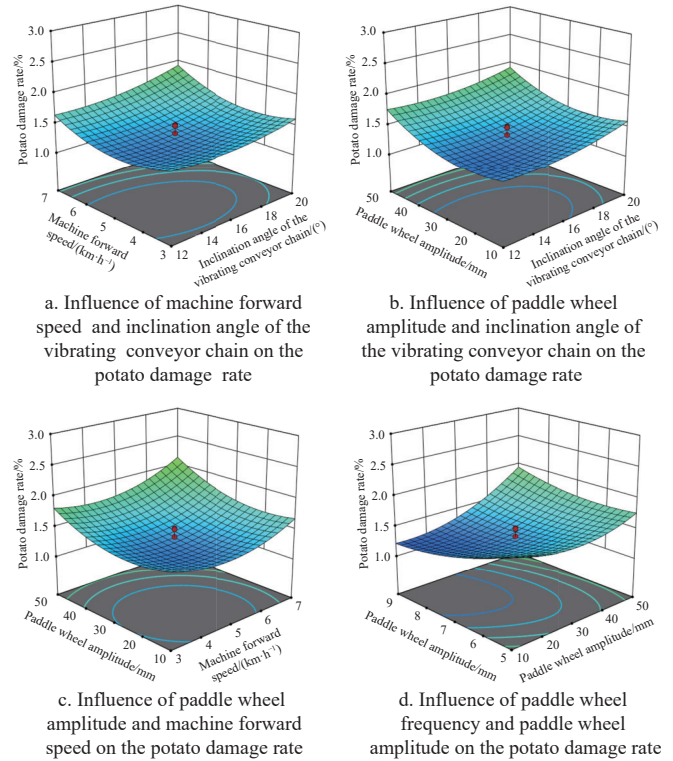


Figure 12 Two-factor influence response surface for potato damage rate

4 Field tests

4.1 Experimental instruments and equipment

To validate the operational efficacy of the aforementioned data, field verification trials were conducted using a 3110G self-propelled potato harvester at a potato cultivation base in Dingxi, Gansu Province. The experimental field featured a double-row planting system per ridge in loess soil (Yellow Cotton soil). Soil moisture content was determined by randomly collecting five replicate samples from the 0-20 cm cultivated layer, followed by the oven-drying method (GB/T 50123-2019, Standard for Soil Test Methods). After excluding outliers, the average soil moisture content was measured as 13%±1.2% (mean ± standard deviation). Key agronomic parameters were quantified using a measuring tape: Ridge width: 800 mm, Intra-ridge row spacing: 150 mm, Plant spacing: 250 mm.

Potato-soil separation efficiency and potato damage rate were used as test indicators. Ten experiments were conducted in the test field, with each experiment covering a distance of 50 m. The results were averaged. The field harvesting experiment is shown in Figure 13.



Figure 13 Field tests

4.2 Experimental indicators

According to clause 6.3.1.8 of the “Technical Specifications for Quality Rating of Potato Harvesters NY/T648-2015” issued by the Ministry of Agriculture of the People’s Republic of China, the formula for calculating the potato damage rate is:

$$L_1 = \frac{Q_1}{Q} \times 100\% \quad (10)$$

where, L_1 is the potato-soil separation efficiency, %; Q_1 is the mass of potatoes entering the lifting device, kg; and Q is the total mass of potatoes and soil entering the lifting device, kg.

$$T_1 = \frac{W_1}{W} \times 100\% \quad (11)$$

where, T_1 is the potato-soil separation efficiency, %; W_1 is the mass of potatoes entering the lifting device, kg; and W is the total mass of potatoes and soil entering the lifting device, kg.

The calculating equation for the mean relative error (MRE) is defined as:

$$MRE = \frac{1}{n} \sum_{i=1}^n \left| \frac{x_i - u}{u} \right| \times 100\% \quad (12)$$

where, MRE represents the mean relative error between simulation data and field experimental data, %; n is the number of experimental trials; i denotes the measured value from the i -th simulation; and u corresponds to the field experimental measurement.

4.3 Experimental results and analysis

According to the “Q/0781QHL01-2019 Potato harvester” enterprise standard, the average potato-soil separation efficiency is 96% and the average damage rate is 2%. A comparative analysis demonstrated that the mean relative errors between the simulation data and field experimental data were 0.47% and 0.3%, respectively. These exceptionally low discrepancies confirm the high fidelity of the simulation model in replicating real-world conditions. The strong consistency between numerical predictions and empirical measurements rigorously validates the accuracy and robustness of the proposed computational framework. This alignment underscores the model’s suitability for practical agricultural applications.

5 Conclusions

1) The efficiency of potato-soil separation and minimization of the extent of potato damage are crucial for efficient and damage-free potato harvesting. Analysis of potato movement on the conveyor chain identified the inclination angle of the conveyor

chain, machine movement speed, beater wheel amplitude, and beater wheel frequency as key factors affecting efficient and damage-free potato harvesting.

2) By combining RecurDyn-EDEM to construct a coupled simulation model of the soil-potato-conveyor system, multiple regression equations were obtained to determine the effects of conveyor inclination angle, machine movement speed, beater wheel amplitude, and beater wheel frequency on potato-soil separation efficiency and potato damage. The order of influence on soil content was: machine forward speed > paddle wheel frequency > paddle wheel amplitude > inclination angle of the vibrating conveyor chain. The order of influence on damage rate was: paddle wheel amplitude > paddle wheel frequency > machine forward speed > inclination angle of the vibrating conveyor chain. Using Design-Expert 12 software for optimization, the optimal parameters were determined to be inclination angle of the vibrating conveyor chain of 18°, machine forward speed of 4.739 km/h, paddle wheel amplitude of 32.835 mm, and beating wheel frequency of 6.004 Hz.

3) The simulation model parameters were validated through field experiments. The results showed an average potato-soil separation efficiency of 96% and an average damage rate of 2%, which were consistent with the coupled simulation results, meeting the experimental requirements.

Acknowledgements

We acknowledge that this work was financially supported by the National Natural Science Foundation of China (Grant No. 52265029), National Modern Agricultural Industrial Technology System Project (Grant No. CARS-09-P32), and Hainan Postgraduate Innovation Project in 2024 (Grant No. Qhyb2024-20).

[References]

- National Bureau of Statistics of China. China Agricultural Statistical Yearbook. Beijing: China Statistics Press, 2023. (in Chinese)
- Yang R B, Tian G B, Shang S Q, Wang B J, Zhang J, Zhai Y M. Design and experiment of roller group soil-potato separation device for potato harvester. *Transactions of the CSAM*, 2023; 54(2): 107–118.
- Wang X Y, Lyu D Y, Ren J Y, Zhang M, Meng P X, Li X Q. Development of cleaning device for bagging potato combine harvester. *Transactions of the CSAE*, 2022; 38(S1): 8–17.
- Lü J Q, Du C L, Liu Z Y, Li J C, Li Z H, Li Z Y. Design and experiment of impurity removal device for potato hopper. *Transactions of the CSAM*, 2021; 52(1): 82–90, 61.
- Shi M M, Wei H A, Liu X, Hu Z Q, Yang X P, Sun G H. Development status of potato harvesting machinery at home and abroad. *Journal of Agricultural Mechanization Research*, 2013; 35(10): 213–217.
- Wang H Y. Design and experiment of self-propelled potato combine harvester for mountainous areas. Master’s thesis, Kunming University of Science and Technology, 2021. DOI: [10.27200/d.cnki.gkmlu.2021.001808](https://doi.org/10.27200/d.cnki.gkmlu.2021.001808). (in Chinese)
- Yang H G, Hu Z C, Wang B, Peng B L, Wang G P. Research progress of mechanized potato harvesting technology. *Journal of Chinese Agricultural Mechanization*, 2019; 40(11): 27–34.
- Song L J, Liu W Y, Wu H F, Gao T, Hao W F. Characteristics of soil nutrients and their relationship with soil microbial properties in *Artemisia sacrorum* communities in the loess hilly region. *Int J Agric & Biol Eng*, 2018; 11(4): 127–134.
- Zhang X Y, Zhang R, Wang J W, Tang X J, Zhang Z R, Wei P C. Effects of environmentally friendly plastic film mulching on soil nutrient environment and maize yield in central Gansu. *Water Saving Irrigation*, 2023; 10: 55–60, 74.
- Azizi P, Sakenian Dehkordi N, Farhadi R. Design, construction and evaluation of potato digger with rotary blade. *Cercetări Agronomice în Moldova*, 2014; 47(3): 71–82.
- Opăru L, Pathare P B. Bruise damage measurement and analysis of fresh horticultural produce: A review. *Postharvest Biology & Technology*, 2014;

91(5): 9–24.

[12] Van Canneyt T, Tijskens E, Ramon H, Verschoore R, Sonck B. Characterisation of a potato-shaped instrumented device. *Biosystems Engineering*, 2003; 86(3): 275–285.

[13] Li T, Yang M L, Zhang X, Zhang E G, Cheng X T, Wang X L. Research on mechanized potato production technology and regional differences in Northwest China. *Transactions of the CSAM*, 2020; 51(S1): 307–313.

[14] Yin Y Y, Wang Z Z, Yang R B, Wang J, Wang Z C. Simulation analysis and parameter optimization of conveyor chain in potato harvester. *Journal of Agricultural Engineering*, 2020; 10(10): 79–83.

[15] Shen H Y, Wang B, Wang G P, Wang Y M, Bao G C, Hu L L, et al. Research and optimization of the hand-over lifting mechanism of a sweet potato combine harvester based on EDEM. *Int J Agric & Biol Eng*, 2023; 16(5): 71–79.

[16] Xin L L, Liang J H. A dynamic analysis on the potato conveying and separation system considering the acting force of a material. *Transactions of FAMENA*, 2019; 43(SII): 35–42.

[17] Wei Z C, Li H W, Mao Y J, Sun C Z, Li X Q, Liu W Z, et al. Experiment and analysis of potato-soil separation based on impact recording technology. *Int J Agric & Biol Eng*, 2019; 12(5): 71–80.

[18] Wei Z C, Su G L, Li X Q, Wang F M, Sun C Z, Meng P X. Parameter optimization and experiment of wavy screen surface for potato harvester based on discrete element method. *Transactions of the CSAM*, 2020; 51(10): 109–122.

[19] Yang R B, Zhang J, Shang S Q, Tian G B, Zhai Y M, Pan Z G. Design and experiment of secondary conveying and separating device for sweet potato combine harvester. *Journal of Jilin University: Engineering and Technology Edition*, 2023; 54(9): 2708–2722.

[20] Chen M D, Liu X T, Hu P X, Zhai X T, Han Z L, Shi Y L, et al. Study on rotor vibration potato-soil separation device for potato harvester using DEM-MBD coupling simulation. *Computers and Electronics in Agriculture*, 2024; 218: 108638.

[21] Wang X H, Wei Z C, Su G L, Meng P X, Wang F M, Zhang X C, et al. Design and experiment of disturbance separation device for potato harvester. *Transactions of the CSAM*, 2024; 55(4): 101–112.

[22] Yan D M, Xu J, Zhang Z F. Design and analysis of a vibratory separation screen for potato harvesters. *Journal of Gansu Agricultural University*, 2022; 57(4): 220–226.

[23] Feng B, Wang H C, Wang G P, Sun W, Shi L R, Tian B. Optimization and experiment of operational parameters for the separation sieve of a small potato harvester. *Journal of Agricultural Mechanization Research*, 2024; 46(10): 138–144,152.

[24] Beznosyuk R V, Evtekhov D V, Borychev S N, Kostenko M Y, Rembalovich G K. Justification of parameters of a finger hump of potato harvesters when vibrating canvas. *IOP Conference Series: Earth and Environmental Science*, 2022; 981(4): 042051.

[25] Hrushetskiy S, Omelyanov O. Justification of the main design parameters of the rotary working body of root harvest machines. *Engineering, Energy, Transport AIC*, 2022; 1: 2.

[26] Issa I M, Zhang Z, El-Kolaly W, Yang X, Wang H. Design, ANSYS analysis and performance evaluation of potato digger harvester. *International Agricultural Engineering Journal*, 2020; 29(1): 60–73.

[27] Lü J Q, Sun H, Dui H, Peng M M, Yu J Y. Design and experiment on conveyor separation device of potato digger under heavy soil condition. *Transactions of the CSAM*, 2017; 48(11): 146–155.

[28] Chen Z, Duan H, Cai X, Wang J, Xu T, Yu C, et al. Distribution characteristics of potato contact stress during the drop impact. *Journal of South China Agricultural University*, 2020; 41(5): 99–108.

[29] Wei Z C, Wang Y W, Li X Q, Wang J M, Su G L, Meng P X, et al. Design and experiments of the potato combine harvester with elastic rubbing technology. *Transactions of the CSAE*, 2023; 39(14): 60–69.

[30] Wang L J, Zhou B, Wan C, Zhou L. Structural parameter optimization of a furrow opener based on EDEM software. *Int J Agric & Biol Eng*, 2024; 17(3): 115–120.

[31] Wang F Y, Zhang W X, Jiang J T. Seed guide path planning and parameter optimization for air-suction carrot seedmetering device. *Int J Agric & Biol Eng*, 2023; 16(5): 104–112.

[32] Li J R. Study on the crushing and separation characteristics of potato-soil aggregates. Doctoral dissertation, Inner Mongolia Agricultural University, 2023. DOI: [10.27229/d.cnki.gnmnu.2023.000511](https://doi.org/10.27229/d.cnki.gnmnu.2023.000511). (in Chinese)

[33] Wang F Y, Qiu Z C, Pan Y F, Sun G Q. DEM-based parameter optimization and tests of digging green onions. *Int J Agric & Biol Eng*, 2023; 16(4): 126–133.

[34] Tong Z W, Li L H, Zhang X L, Chen Y, Liu X C, Zhou P L, et al. Design and experiment of the components for soil flow direction control of hillling machine based on EDEM. *Int J Agric & Biol Eng*, 2022; 15(3): 122–131.

[35] Zhou J Q. Design and performance test of potato picking device based on discrete element method (Master's thesis). Inner Mongolia Agricultural University, 2023. DOI: [10.27229/d.cnki.gnmnu.2023.001303](https://doi.org/10.27229/d.cnki.gnmnu.2023.001303). (in Chinese)

[36] Zhang W X, Wang F Y. Parameter calibration of American ginseng seeds for discrete element simulation. *Int J Agric & Biol Eng*, 2022; 15(6): 16–22.

[37] Deb K, Pratap A, Agarwal S, Meyarivan T. A fast and elitist multiobjective genetic algorithm: NSGA-II. *IEEE Transactions on Evolutionary Computation*, 2002; 6(2): 182–197.